Title
Representing leaf and root physiological traits in CLM improves global carbon and nitrogen cycling predictions

Journal
Journal of Advances in Modeling Earth Systems, 8(2)

ISSN
1942-2466

Authors
Ghimire, Bardan
Riley, William J
Koven, Charles D
et al.

Publication Date
2016-06-01

DOI
10.1002/2015ms000538

Peer reviewed

AGU PUBLICATIONS

Journal of Advances in Modeling Earth Systems

RESEARCH ARTICLE

10.1002/2015MS000538

Key Points:
- Improved representation of root and leaf physiological traits in Community Land Model
- Model changes led to an overall improvement in global carbon cycling predictions
- Model improved with mechanistic leaf-level nitrogen allocation and root nitrogen uptake kinetics

Supporting Information:
- Supporting Information S1

Correspondence to:
B. Ghimire,
bghimire@lbl.gov

Citation:
Ghimire, B., W. J. Riley, C. D. Koven, M. Mu, and J. T. Randerson (2016), Representing leaf and root physiological traits in CLM improves global carbon and nitrogen cycling predictions, *J. Adv. Model. Earth Syst.*, *8*, 598–613, doi:10.1002/2015MS000538.

Received 25 AUG 2015
Accepted 12 MAR 2016
Accepted article online 18 MAR 2016
Published online 1 MAY 2016

Representing leaf and root physiological traits in CLM improves global carbon and nitrogen cycling predictions

Bardan Ghimire[1], William J. Riley[1], Charles D. Koven[1], Mingquan Mu[2], and James T. Randerson[2]

[1]Earth Sciences Division, Lawrence Berkeley National Laboratory, Berkeley, California, USA, [2]Department of Earth System Science, University of California, Irvine, California, USA

Abstract In many ecosystems, nitrogen is the most limiting nutrient for plant growth and productivity. However, current Earth System Models (ESMs) do not mechanistically represent functional nitrogen allocation for photosynthesis or the linkage between nitrogen uptake and root traits. The current version of CLM (4.5) links nitrogen availability and plant productivity via (1) an instantaneous downregulation of potential photosynthesis rates based on soil mineral nitrogen availability, and (2) apportionment of soil nitrogen between plants and competing nitrogen consumers assumed to be proportional to their relative N demands. However, plants do not photosynthesize at potential rates and then downregulate; instead photosynthesis rates are governed by nitrogen that has been allocated to the physiological processes underpinning photosynthesis. Furthermore, the role of plant roots in nutrient acquisition has also been largely ignored in ESMs. We therefore present a new plant nitrogen model for CLM4.5 with (1) improved representations of linkages between leaf nitrogen and plant productivity based on observed relationships in a global plant trait database and (2) plant nitrogen uptake based on root-scale Michaelis-Menten uptake kinetics. Our model improvements led to a global bias reduction in GPP, LAI, and biomass of 70%, 11%, and 49%, respectively. Furthermore, water use efficiency predictions were improved conceptually, qualitatively, and in magnitude. The new model's GPP responses to nitrogen deposition, CO_2 fertilization, and climate also differed from the baseline model. The mechanistic representation of leaf-level nitrogen allocation and a theoretically consistent treatment of competition with belowground consumers led to overall improvements in global carbon cycling predictions.

1. Introduction

Land surface processes impact climate [*Foley et al*., 1998; *Sellers et al*., 1986] and are impacted by climate [*Bonan*, 2008], forming complex feedbacks critical to climate change [*Friedlingstein et al*., 2006; *Gregory et al*., 2009]. The land surface components of Earth System Models (ESMs) have evolved from only representing biophysical processes (i.e., hydrology and energy cycling) to including ecosystem carbon cycling, vegetation dynamics, and nutrient cycling [*Oleson et al*., 2013; *Sitch et al*., 2003; *Wang et al*., 2010]. Ecosystem nitrogen cycling is a dominant driver of terrestrial carbon-climate interactions through its impacts on vegetation growth and productivity [*Reich et al*., 2006] and microbial decomposition of organic matter [*Hu et al*., 2001].

Plant carbon uptake and carbon release by microbial decomposition depend on nitrogen use efficiency and the relative competitiveness of plants and microbes to acquire nitrogen [*Kaye and Hart*, 1997]. Model prediction of future ecosystem responses to nitrogen cycling is highly uncertain due to model uncertainties in representation of nitrogen deposition impacts on carbon cycling [*Matson et al*., 2002] and representation of high latitude systems that store large reservoirs of carbon and nitrogen in permafrost soils [*Jonasson et al*., 1999].

Current land surface models have large uncertainties in predicting historical and current carbon exchanges [*Beer et al*., 2010; *Zaehle et al*., 2014]. The difference in predictions of ESM-scale land models has been attributed to many factors, including model structural differences (in represented processes and the large diversity of represented processes), inclusion or exclusion of nutrient limitations on productivity, and uncertainties in model parameters [*Huntzinger et al*., 2013; *Schaefer et al*., 2012]. One of the most important photosynthetic model parameters, the maximum carboxylation rate by the Rubisco enzyme (V_{cmax}; which varies by plant functional type [*Kattge et al*., 2009]), has a large range across the models [*Farquhar et al*., 1980; *Rogers*, 2014]. Model

predictions of plant productivity are highly sensitive to V_{cmax} and large variation in predictions of carbon sinks is partly attributed to the variations of V_{cmax} amongst models [*Rogers*, 2014].

In many ecosystems, nitrogen is an important nutrient limiting plant growth and productivity, especially in nitrogen poor younger soils in high latitudes [*LeBauer and Treseder*, 2008; *Vitousek and Howarth*, 1991]. Plants require nitrogen as essential components of photosynthetic proteins involved in light capture, electron transport, and carboxylation [*Evans*, 1989a, 1989b]. Nitrogen is also an important constituent of mitochondrial enzymes that regulate respiration and ATP generation [*Makino and Osmond*, 1991]. Although nitrogen is an important regulator of photosynthetic and respiratory processes, those ESMs which do include N cycles lack mechanistic representation of key processes linked to plant nitrogen cycling, including the role of root traits in plant nitrogen uptake, and linkages among leaf nitrogen, photosynthetic parameters (e.g., V_{cmax}), and photosynthesis rates [*Zaehle et al*., 2014].

Zaehle et al. [2014] describe two classes of terrestrial ecosystem model coupling between N and photosynthetic C uptake: "instantaneous downregulation," and "foliar N content." The instantaneous downregulation approach is based on the idea that a potential photosynthesis can be calculated initially without considering N limitations, and then downregulated to an actual photosynthesis rate once N availability is known and considering the N required to balance stoichiometric relationships within tissues and new photosynthesis. One such instantaneous downregulation model is the Community Land Model, in versions starting from CLM-CN [*Thornton et al*., 2007] through CLM 4.5 [*Oleson et al*., 2013]. In contrast, the foliar N content models work on the principle that leaf N content determines photosynthesis rates; limitation occurs because leaf N content is reduced to maintain stoichiometric relationships when allocating C to tissues, and this reduction in foliar N then reduces photosynthesis.

The instantaneous downregulation approach is conceptually problematic. Plants do not photosynthesize at potential rates and then downregulate; so it is not possible to identify an observable quantity that corresponds to model predictions of potential photosynthesis. It is therefore difficult to assess the realism of the model predictions of N limitation, or diagnose the magnitude of N limitation in the model versus observations. These structural problems in estimating potential photosynthesis provide rationale for determining leaf nitrogen and its impacts on emergent photosynthetic parameters and rates via the foliar N content approach [e.g., *Zaehle and Friend*, 2010]. Unlike the instantaneous downregulation approach, the foliar N content approach allows direct comparison between observable quantities (e.g., foliar N content and photosynthesis rates) to parameterize, test, and improve model structures. The foliar N content approach also allows for direct comparisons to N manipulation experiments, including model comparisons with tissue concentration and NPP measurements.

In addition to problems associated with estimating photosynthesis and the instantaneous downregulation approach, the role of plant roots in nutrient acquisition have largely been ignored in Earth System models. For example, in CLM4.5, nitrogen uptake is scaled based on leaf level processes (e.g., primary productivity) rather than root scale process, with competitive distribution of soil nitrogen between plants and other consumers assumed to be proportional to their relative nitrogen demands [*Thornton et al*., 2007]. However, we believe root-scale processes are essential for understanding plant nitrogen cycling, as root physiology plays an important role in root nutrient uptake by regulating root biomass, surface area, mycorrhizal associations that facilitate nutrient acquisition, priming, and nutrient uptake efficiency [*Miller and Cramer*, 2005; *Pate*, 1973; *Read and Perez-Moreno*, 2003]. Root nutrient uptake efficiency is affected by plant processes involved in removing adsorbed nutrients, maintaining ionic gradients for nutrient diffusion, and producing transporter molecules that bind to and transport nutrients from soil to roots. Models have represented these processes by lumping these terms as parameters in the Michaelis Menten equation [*Grant et al*., 2010; *Thomas et al*., 2013].

This paper presents a new nitrogen-carbon coupling model for CLM, shifting it from the instantaneous downregulation approach to the foliar N content paradigm, and from a leaf-centric to a root-centric N uptake paradigm, by improving representation of (1) plant nitrogen uptake based on root scale Michaelis-Menten kinetics; (2) linkages between leaf nitrogen and plant productivity based on observations in the global TRY database and several individual studies; (3) plant nitrogen allocation; and (4) specific leaf area canopy profiles. After describing the new model structure, we compare model predictions of GPP, LAI, biomass, and evapotranspiration with observations, evaluate overall model performance with the International Land

Model Benchmarking Project (ILAMB) benchmarking tool [*Luo et al*., 2012], and present relative improvements compared to the baseline CLM4.5 version of the model. In the remainder of the paper, we refer to the baseline model as CLM4.5 and the new version as CLM4.5*.

2. Materials and Methods

2.1. Plant Nitrogen Uptake

In CLM4.5, plant nitrogen demand (NF_{plant_demand} (gN m^{-2} s^{-1})) is proportional to assimilated carbon available to be allocated for new growth (CF_{avail_alloc} (gC m^{-2} s^{-1})) [*Oleson et al*., 2013]:

$$NF_{plant\_demand} = CF_{avail\_alloc} \frac{N_{allom}}{C_{allom}} \tag{1}$$

where N_{allom}/C_{allom} (gN gC^{-1}) is the plant level nitrogen to carbon stoichiometry for new growth, and is calculated for each plant functional type based on prescribed carbon to nitrogen ratios (C:N) for each plant part. CF_{avail_alloc} is estimated as:

$$CF_{avail\_alloc} = CF_{GPPpot} - CF_{GPP,mr} - CF_{GPP,xs} \tag{2}$$

where CF_{GPPpot}, $CF_{GPP,mr}$, and $CF_{GPP,xs}$ (gC m^{-2} s^{-1}) are the carbon fluxes associated with potential *GPP*, maintenance respiration, and carbon flux to the storage pool, respectively. Maintenance respiration is estimated as a function of leaf nitrogen content and temperature, and growth respiration is estimated as a fixed factor (0.3) of the nitrogen allocated to new growth. Further details of the calculation of maintenance and growth respiration is provided in *Oleson et al*. [2013]. In CLM4.5, plants and (implicit) microbial SOM decomposition compete for mineral nitrogen based on the magnitude of their relative demands. Plant nitrogen uptake (NF_{plant_uptake} (gN m^{-2} s^{-1})) is estimated from plant nitrogen demand after accounting for competition with SOM decomposition. After plant nitrogen and microbial immobilization are accounted for, the remaining mineral N can then be nitrified or denitrified, and finally becomes available for leaching.

In our new model formulation, which we view as an interim step toward a more mechanistic treatment of terrestrial N cycling, we implemented the Michaelis-Menten [*Michaelis and Menten*, 1913] equation for estimating root nitrogen uptake competitiveness in a manner similar to that proposed by *Thomas et al*. [2013]. This approach is an interim solution to a comprehensive model structure because we impose a second round of competition based on root nitrogen uptake competitiveness and other nitrogen consumers (e.g., heterotrophic decomposers, denitrifiers, nitrifiers) via the standard relative-demand-based downregulation. Future work will include integrating a new approach, called the Equilibrium Chemistry Approximation (ECA) [*Tang and Riley*, 2013, 2015; *Zhu et al*., 2015], which combines the Michaelis-Menten theory with a generic approach to represent competition between consumers for substrates. In the modified model, CLM4.5*, plant nitrogen uptake competitiveness (NF_{uptake} (gN m^{-2} s^{-1})) is estimated as:

$$NF_{uptake} = U_{Nmax} CS_{froot} \frac{NS_{smin}}{K_{smin} + NS_{smin}} S_N S_T \tag{3}$$

where U_{Nmax} (2.7×10^{-8} gN gC^{-1} s^{-1}) [*Thomas et al*., 2013] is maximum nitrogen uptake per root biomass at 25°C, CS_{froot} (gC m^{-2}) is root biomass, NS_{smin} (gN m^{-2}) is mineral soil nitrogen, K_{smin} (=1 gN m^{-2}) [*Thomas et al*., 2013] is a half saturation constant, S_N is the nitrogen demand scalar, and S_T is the temperature scalar for nitrogen uptake. The Michaelis-Menten kinetics (i.e., equation (3)) combines plant and microbial nitrogen demand to calculate plant nitrogen uptake and microbial immobilization based on their relative demands and soil mineral nitrogen availability. The Michaelis-Menten kinetics used for modeling root nitrogen uptake improves upon previous ESMs, which do not incorporate root physiological characteristics in simulating nitrogen uptake. However in future studies we will further improve our approach by (1) incorporating dynamic nitrogen uptake proportional to root surface area (rather than root biomass), (2) optimizing root architectural characteristics across soil depth in response to soil mineral nitrogen supply, and (3) representing the role of mycorrhizal-root interacts in nitrogen uptake [*McCormack et al*., 2015; *McMurtrie et al*., 2012; *Smithwick et al*., 2014; *Warren et al*., 2015]. The distinction between root mass and surface area does not impact our study because the two scale linearly with each other. Root mass and surface area linearly scale if we assume that shape of roots are cylindrical, comprising two populations of fine and coarse roots with constant diameter and fixed proportion of fine to coarse roots. Roots also have different

functions, transporter densities and enzyme production, and the use of K_{smin} in the Michaelis-Menten equation attempts to simplify these complex interactions by subsuming all these complexities into a constant competitiveness parameter.

S_N ranges from 0 to 1 and is computed as:

$$S_N = \frac{CN_{leaf} - CN_{leaf\_min}}{CN_{leaf\_max} - CN_{leaf\_min}} \tag{4}$$

CN_{leaf_min} (gC gN^{-1}) and CN_{leaf_max} (gC gN^{-1}) are the minimum and maximum leaf C:N, respectively, and encompass the range of variation in leaf C:N (CN_{leaf}). In CLM4.5*, we incorporate a flexible leaf C:N with the CN_{leaf_min} and CN_{leaf_max} varying within a range of $\pm$10gC gN^{-1} of the central CN_{leaf} value. Since CN_{leaf} is prescribed for different plant functional types, CN_{leaf_min} and CN_{leaf_max} vary by plant functional type. This range of variation of CN_{leaf} is similar in magnitude to values used in other ecosystem models [*Zaehle and Friend*, 2010] and previous studies [*Reich et al*., 1997]. However in future versions of CLM we are working on improving this range based on CN_{leaf} values reported in the TRY database [*Kattge et al*., 2011].

S_T is the temperature scalar for the top soil layer, and is similar to the temperature scalar for decomposition in CLM4.5 [*Oleson et al*., 2013]:

$$S_T = Q_{10}^{\left(\frac{T_{soil} - T_{ref}}{10}\right)} \tag{5}$$

where T_{soil} (°C) is soil temperature, T_{ref} (=25°C) is the reference temperature, and Q_{10} is set to a constant value of 1.5. We note that recent work suggests that a constant value for Q_{10} may be unrealistic and can cause biases in predictions of soil organic carbon dynamics [*Tang and Riley*, 2015].

2.2. Nitrogen Limitation on Photosynthesis

Nitrogen limitation on photosynthesis is determined in CLM4.5 by downregulating (i.e., reducing) potential GPP (CF_{GPPpot}) (gC m^{-2} s^{-1}) if soil nitrogen is limiting. The downregulated GPP (CF_{GPP}) (gC m^{-2} s^{-1}) is estimated as:

$$CF_{GPP} = CF_{GPPpot} f_{dreg} \tag{6}$$

where f_{dreg} (ranging from 0 to 1) is the downregulation factor, which depends on the plant nitrogen demand required to support potential GPP and competition for mineral soil nitrogen between (inferred) microbial decomposition and plants.

CF_{GPPpot} is estimated from the coupled Farquhar and Ball Berry stomatal conductance models [*Farquhar et al*., 1980]. The Farquhar model relies on two key parameters: maximum carboxylation rate by the Rubisco enzyme at 25°C (V_{cmax25}) (μmol CO_2 (m leaf)$^{-2}$ s^{-1}) and maximum electron transport rate at 25°C (J_{max25}) (μmol electron (m leaf)$^{-2}$ s^{-1}). In CLM4.5 (*Bonan et al*. [2011]), V_{cmax25} is prescribed as a constant for different plant functional types based on *Kattge et al*. [2009]:

$$V_{cmax25} = N_a F_{LNR} F_{NR} a_{R25} \tag{7}$$

where N_a (g N (m leaf)$^{-2}$) is the leaf nitrogen content per area, F_{LNR} is the fraction of leaf nitrogen in Rubisco, F_{NR} is the ratio of the molecular mass to nitrogen content of Rubisco (g Rubisco (g N in Rubisco)$^{-1}$), and a_{R25} (μmol CO_2 (g Rubisco)$^{-1}$ s^{-1}) is the specific activity of Rubisco at 25°C. N_a is estimated from leaf C:N (CN_L) and specific leaf area at top of canopy (SLA_0) [*Thornton and Zimmermann*, 2007]:

$$N_a = \frac{1}{CN_L SLA_0} \tag{8}$$

Since CN_L (gC leaf (gN leaf)$^{-1}$), SLA ((m leaf)^2 (gC leaf)$^{-1}$), F_{LNR}, F_{NR}, and a_{R25} are constants for a given plant functional type, V_{cmax25} is also a constant for each plant functional type. However, in CLM4.5, V_{cmax25} varies with canopy depth due to canopy depth dependence of specific leaf area (SLA m^2 m^{-2}), but this variation is unrelated to leaf nitrogen content. Although CLM4.5 represents plant nitrogen pools, N_a is not predicted based on root nitrogen uptake, but rather is computed using equation (8) and so is constant in time for each plant functional type. Therefore, plant nitrogen allocated to the leaf does not play a functional role in estimating photosynthesis in CLM4.5. Since V_{cmax25} is used to estimate potential GPP, the V_{cmax25} used in

CLM4.5 is a potential rate. We note that the potential V_{cmax25} may be inconsistent with field observations that are obtained from A-C_i curves under conditions that may be inconsistent with a maximum rate.

In CLM4.5, J_{max25} is computed as a function of V_{cmax25} based on *Kattge and Knorr* [2007]:

$$\frac{J_{max25}}{V_{cmax25}} = 2.59 - 0.035(T_{10} - T_f)$$

where T_{10} is the 10 day mean air temperature (K) and T_f is the freezing point of water (K).

To allow V_{cmax25} to vary with leaf nitrogen content, following the "foliar N content" paradigm, we modified CLM4.5 by integrating a model structure where leaf nitrogen explicitly regulates V_{cmax25} (and therefore J_{max25}). In the modified model, V_{cmax25} is estimated from leaf nitrogen (NS_{leaf}) (gN leaf (m leaf)$^{-2}$) as:

$$V_{cmax25} = a + b\ NS_{leaf} \tag{9}$$

where a and b are plant functional types (PFT)-specific intercepts and slope, respectively, derived from observations in the TRY database [*Kattge et al.*, 2009]. In the modified model, NS_{leaf} (gN leaf (m leaf)$^{-2}$) is a prognostic variable predicted based on carbon allocation and the leaf C:N ratio. As a result, V_{cmax25} in the modified model is a dynamic emergent trait varying with leaf nitrogen content, which itself depends on root uptake traits and therefore the soil biogeochemical competitive environment. We further scaled V_{cmax25} by the day length multiplier (which represents the seasonal variation in V_{cmax}) as implemented in CLM4.5.

2.3. Plant Nitrogen Allocation and Flexible C:N Ratio

Nitrogen allocation to different plant parts in CLM4.5 depends on the carbon allocation and C:N of the given plant part. C:N in CLM4.5 is a prescribed constant for a given plant functional type [*Thornton and Zimmermann*, 2007]. We modified CLM4.5 by incorporating a new model structure with a flexible C:N where the leaf pool is allocated the residual nitrogen after the nitrogen demands of different plant organs (e.g., fine root and wood) are satisfied. We implemented this simpler allocation scheme to incorporate flexible leaf C:N while attempting to keep the C:N of other plant parts fixed. We have also implemented an alternative allocation scheme for the next version of CLM, which allocates nitrogen to different plant parts based on the relative demand of the respective plant part allowing C:N of all plant parts to vary simultaneously.

Plant nitrogen allocation to different plant organs ($NF_{alloc,o}$ (gN m^{-2} s^{-1})) is calculated from the balance of supply of nitrogen available to the plant and nitrogen demand of a given plant organ as:

$$NF_{alloc,o} = \min\left(NF_{demand,o}, NF_{supply,o}\right) \tag{10}$$

where $NF_{demand,o}$ (gN m^{-2} s^{-1}) and $NF_{supply,o}$ (gN m^{-2} s^{-1}) are nitrogen demand and supply, respectively, for plant organ o. $NF_{demand,o}$ is estimated from the carbon allocation and C:N of the given plant organ as:

$$NF_{demand,o} = \frac{CF_{alloc,o}}{CN_o} \tag{11}$$

where $CF_{alloc,o}$ (gC m^{-2} s^{-1})) is the carbon flux allocated to the given plant organ before tissue construction costs are estimated for building the plant part and CN_o (gC gN^{-1}) is the C:N of the given plant organ.

2.4. Prognostic Leaf Area Index

CLM4.5 predicts Leaf Area Index (LAI ((m leaf)^2 (m ground)$^{-2}$)) at each level in the canopy based on leaf carbon content (CS_{leaf} (gC m^{-2})) and specific leaf area (SLA) [*Oleson et al.*, 2013; *Thornton and Zimmermann*, 2007]. SLA is assumed to increase from the top to the bottom of the canopy:

$$SLA(z) = SLA_0 + mz \tag{12}$$

where m is the assumed slope of the relationship between SLA at a given canopy depth (z; measured from canopy top) and at the canopy top (SLA_0). In CLM4.5, m and SLA_0 is specific to each plant functional type. Canopy integrated LAI is computed as:

$$LAI = \frac{SLA_0\left[\exp\left(m * CS_{leaf}\right) - 1\right]}{m} \tag{13}$$

The estimation of *LAI* using an increasing *SLA* profile with canopy depth (equation (12)) is partially responsible for unrealistically high predicted *LAI* in some locations in CLM4.5. To reduce this LAI bias we have removed the increasing SLA profile to a constant SLA across the canopy depth. This LAI bias may also be related to other factors such as over-prediction of GPP. The vegetation related variables, and their definitions and units are outlined in the supporting information.

2.5. Model Simulations

Global CLM4.5 and CLM4.5* simulations were performed with an initial accelerated decomposition spin-up for 1000 years followed by a 200 year spin-up to equilibrate the vegetation and soil pools to steady state conditions [*Koven et al*., 2013]. This model spin-up was forced with year 1850 conditions using meteorological forcing of surface solar radiation, air temperature, and precipitation from *Qian et al*. [2006], nitrogen deposition from *Lamarque et al*. [2005], land-use conditions from *Hurtt et al*. [2006], and carbon dioxide (CO_2) mole fraction. After the spin-up, the model was run from 1850 to 1972 with CO_2, nitrogen deposition, and land use from 1850 to 1972, and recycling surface solar radiation, air temperature, and precipitation from 1948 to 1972. The final model simulation consisted of running CLM4.5 from year 1973 to 2004 using climate [*Qian et al*., 2006] and land-use conditions [*Hurtt et al*., 2006] from year 1973 to 2004. The model simulations for gross primary productivity, carbon stocks, and leaf area index (LAI) were evaluated against data sets from *Beer et al*. [2010], *Saatchi et al*. [2011], and *Zhu et al*. [2013], respectively. We also use the ILAMB package to benchmark the model outputs against reference data using a range of metrics (e.g., bias, root mean square error (RMSE), annual mean and phase) [*Luo et al*., 2012].

We investigated the separate and combined effects of historical CO_2 fertilization and nitrogen deposition by varying, and keeping constant at 1850 levels, CO_2 and nitrogen deposition. We also investigated model predicted LAI using the *Zhu et al*. [2013] data set, and the predicted water use efficiency (WUE) computed as a ratio of GPP and evapotranspiration of CLM4.5 and CLM4.5* using an observationally derived metric based on FLUXNET-MTE [*Beer et al*., 2010; *Jung et al*., 2010].

3. Results

3.1. Impact of Model Changes on Diurnal Cycles

Our changes to the representation of nitrogen dynamics had large impacts on the predicted diurnal cycles of GPP. The conceptual framework a model takes toward representing nutrient (and other resource) competition and losses can have striking impacts on predicted flux exchanges with the atmosphere. To illustrate these impacts at the site level, we have extracted predictions of CLM4.5 and CLM4.5* at specific grid cells from different regions (Figure 1). Recall that, for nutrient controls on GPP, CLM4.5 uses the instantaneous downregulation and relative demand concepts and CLM4.5* uses the new leaf and root trait-based approach with Michaelis-Menten kinetics. The comparison highlights the impacts of nutrient regulation in each model. In CLM4.5, GPP is predicted to have an unrealistic diurnal cycle caused by the instantaneous soil nitrogen limitation and relative demand model structure. These unrealistic responses are absent in CLM4.5* because of the explicit representation of the nitrogen pool available for photosynthesis and the impact of root physiology on plant nitrogen uptake. We note that these unrealistic diurnal cycles in nitrogen constraints on GPP are present in all recent CLM4.5 [e.g., *Koven et al*., 2013; *Riley et al*., 2011] and CLM4.0 [e.g., *Thornton et al*., 2009; *Thornton and Zimmermann*, 2007] simulations that include a prognostic nitrogen cycle.

The diurnal cycle of GPP is driven by diurnal variation of radiation and temperature in both CLM4.5 and CLM 4.5*, but CLM4.5 predicts an unrealistic dip in GPP. The magnitude of the unrealistic dip in CLM4.5-predicted GPP is larger where nitrogen more strongly limits "potential GPP." These results demonstrate that the nitrogen limitation simulated in CLM4.5 (and in CLM4.0) is mechanistically flawed; we discuss below the impact of this problem on inferences of nutrient regulation of carbon-climate feedbacks. In contrast, CLM4.5* does not show the GPP dip because the nitrogen storage in leaves buffers the diurnal nitrogen limitation and the representation of plant nitrogen uptake based on root properties reduces the problem of unrealistic diurnal depletion of soil nitrogen. Moreover, because the N limitation varies continuously with N availability in CLM4.5*, the resulting functional form has less of a threshold behavior than that of CLM4.5, which reduces the potential for such artifacts to occur.

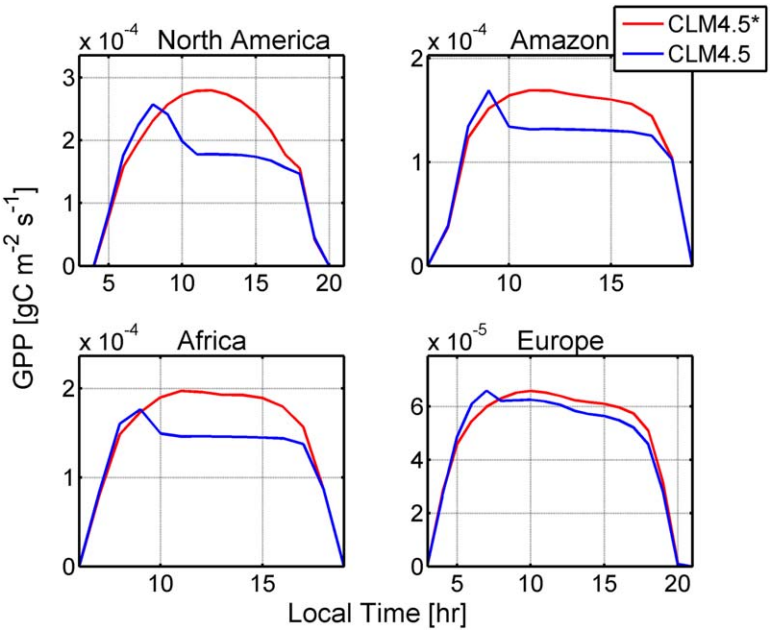

Figure 1. GPP diurnal cycle during growing season showing daytime observations for modified version of CLM4.5 (CLM4.5*) and default version of CLM4.5 (CLM4.5) in different point locations in Eastern North America, Amazon, Africa and Europe. In CLM4.5, GPP is predicted to have an unrealistic dip in the diurnal cycle, which is absent in CLM4.5*. The *x* axis shows the time as daytime observations from the GPP diurnal cycle.

3.2. Impact of Model Changes on Global GPP, Biomass, LAI, and LE

At the global scale, CLM4.5* predictions had lower GPP bias (global GPP bias = 41 gC m^{-2} yr^{-1}) compared to FLUXNET-MTE estimates than did CLM4.5 (global GPP bias= 138 gC m^{-2} yr^{-1}) (Table 1 and Figure 2), corresponding to a reduction in GPP bias of 70% (Table 1). Regional variations exist in the GPP bias between CLM4.5* and CLM4.5 (Figure 2). CLM4.5 over-predicts GPP at high latitudes, especially in North America and Europe. In contrast, CLM4.5* has lower bias in higher latitudes compared to CLM4.5. CLM4.5 over-predicts GPP in the Amazon whereas CLM4.5* under-predicts GPP in the same region.

Across the tropics, CLM4.5* GPP predictions are close to the reference data (FLUXNET-MTE), while CLM4.5 GPP predictions are much higher (Figure 3). In the Southern Hemisphere (taken as 60°S - 30°S), CLM4.5* and CLM4.5 both over predict GPP compared to FLUXNET-MTE. Northern Hemisphere (taken as 30°N - 60°N) GPP predictions were improved in CLM4.5* compared to CLM4.5, but there remains a positive bias.

CLM4.5* also improved biomass predictions compared to CLM4.5 at a global scale (Table 1). Globally, biomass bias was reduced by 49% for the prediction of CLM4.5* (global bias = −0.42 kg C m^{-2}) compared to CLM4.5 (global bias = 0.82 kg C m^{-2}) (Table 1). Regionally, large reductions in CLM4.5* biomass bias occurred in the South American ecosystems.

CLM4.5* also improved predictions of leaf area index compared to CLM4.5. Globally, CLM4.5* has a LAI bias of 1.0, which is lower than the LAI bias of CLM4.5 (global bias = 1.1) by a factor of 11% (Table 1). The largest reductions in LAI bias are in the European and Asian continents (Table 1).

We also computed scoring metrics against reference data for GPP, LAI, and latent heat (LH) using the ILAMB package (Table 2). CLM4.5* performed better in most of the metrics computed by ILAMB compared to CLM4.5. The CLM4.5* overall scores for GPP (=0.78) and LAI (=0.57) are higher than the corresponding CLM4.5 overall scores for GPP (=0.75) and LAI (=0.52). The LH overall scores are similar between CLM4.5 (=0.83) and CLM4.5* (=0.82), although our diurnal cycle analysis (above) indicates that the GPP (and hence LH) fluxes predicted in CLM4.5 are qualitatively inconsistent with observations.

3.3. Impact of Model Changes on PFT-Specific Responses

In addition to regional variations, CLM4.5 and CLM4.5* differ in their predictions for different plant functional types (Figure 4). CLM4.5* has lower GPP bias than CLM4.5 for most plant functional types. In terms of

Table 1. Regional and Global GPP, LAI, and Biomass Bias for Modified Version of CLM4.5 (CLM4.5*) and Default Version of CLM4.5 (CLM4.5)[a]

	CLM4.5 GPP Bias	CLM4.5* GPP Bias	Reduction GPP Bias (%)	CLM4.5 LAI Bias	CLM4.5* LAI Bias	Reduction LAI Bias (%)	CLM4.5 Biomass Bias	CLM4.5* Biomass Bias	Reduction Biomass Bias (%)
Africa	−125	−16	87	0.1	0.3	−283	0.17	−1.00	−502
Asia	275	78	72	1.5	1.1	25	−0.02	−1.02	−5814
Australia	41	128	−214	0.2	0.3	−28	−1.18	−1.10	7
North America	294	127	57	1.7	1.4	16	0.27	0.19	31
Oceania	569	240	58	3.9	2.6	33	2.07	0.32	84
South America	−21	−199	−830	1.5	1.7	−17	5.36	−0.20	96
Europe	362	91	75	2.7	2.1	22	n/a	n/a	n/a
Global	138	41	70	1.1	1.0	11	0.82	−0.42	49

[a]Reference data for GPP and LAI are at a global scale and biomass is available for the tropical regions only. GPP and LAI biases are calculated for years 1995–2004, and biomass bias is calculated for year 2000. GPP bias is in gC m^{-2} yr^{-1}; Biomass bias is in kgC m^{-2}.

the GPP bias magnitudes, CLM4.5's GPP bias is close to or greater than 250 gC m^{-2} yr^{-1} for 11 of the 15 plant functional types, while CLM4.5*'s GPP bias is close to or greater than 250 gC m^{-2} yr^{-1} for 6 of the plant functional types. Amongst the plant functional types, broadleaf deciduous boreal tree has the largest reduction in GPP bias (computed as the difference of CLM4.5* bias and CLM4.5 bias relative to CLM4.5 bias) of 96% followed by broadleaf deciduous boreal shrub (95%) and C3 arctic grass (86%); C_3 non-arctic grass has the largest increase in bias (86%) followed by broadleaf evergreen tropical tree (58%).

The CLM4.5* LAI bias is also lower for all plant functional types, with needleleaf deciduous boreal tree having the largest reduction in bias (computed as the difference of CLM4.5* bias and CLM4.5 bias relative to CLM4.5 bias) of 42% followed by broadleaf deciduous boreal tree (30%); C4 grass and broadleaf deciduous

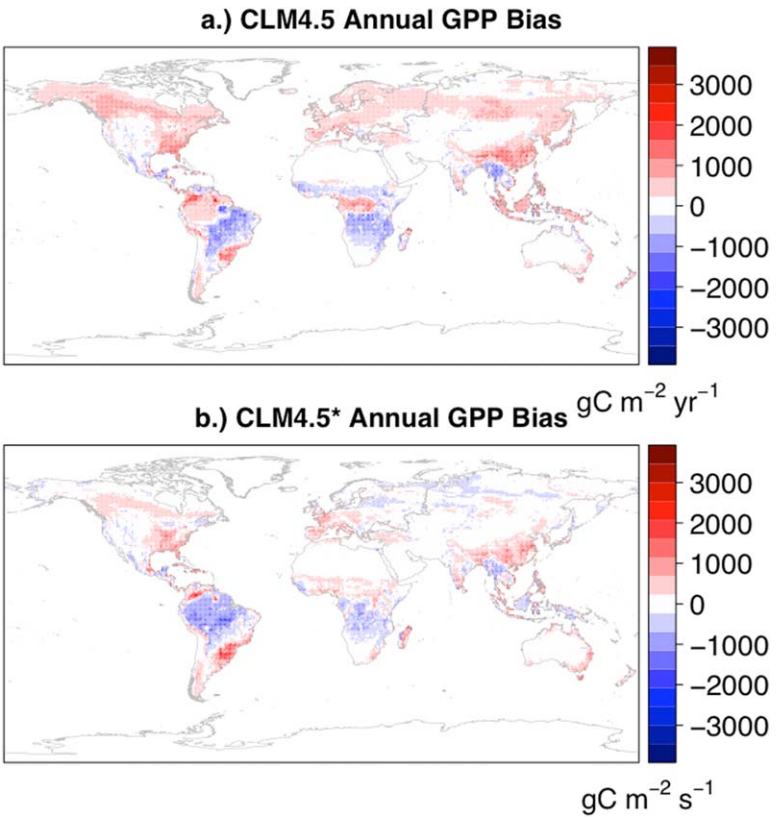

Figure 2. Spatial distribution of the annual GPP bias (=model - reference) for (a) default version of CLM4.5 (CLM4.5) and (b) modified version of CLM4.5 (CLM4.5*) aggregated across 1995–2004. Predictions of CLM4.5* had lower GPP bias compared to FLUXNET-MTE estimates than did CLM4.5, especially in higher latitudes.

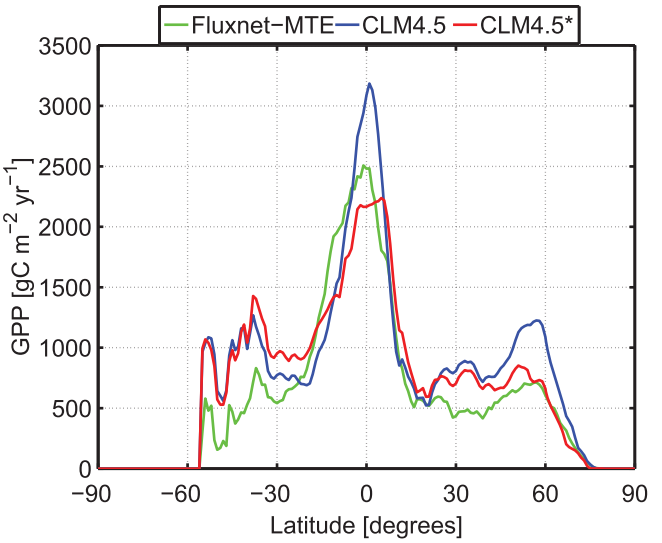

Figure 3. Latitudinal GPP variation for default version of CLM4.5 (CLM4.5) and modified version of CLM4.5 (CLM4.5*) aggregated across 1995–2004. Predictions of CLM4.5* vary by latitude, and is closer to FLUXNET-MTE in the tropics and northern hemisphere compared to CLM4.5.

tropical tree have the largest increase in bias of 74% followed by broadleaf deciduous temperate shrub (35%) (Figure 4).

The overall biomass bias aggregated across plant functional types is lower in CLM4.5* with both broadleaf deciduous temperate tree and broadleaf evergreen tropical tree having the largest reduction in bias relative to CLM4.5 of 89% followed by needleleaf evergreen temperate tree (83%) (Figure 4).

The differences in GPP simulations of CLM4.5 and CLM4.5* are related to differences in plant nitrogen uptake and nitrogen use efficiency (NUE; defined as the ratio of GPP and plant nitrogen uptake (Figure 5)). GPP is proportional to both NUE and nitrogen uptake. CLM4.5* has higher NUE for most plant functional types (except for tropical forests), but the higher NUE is compensated by lower plant nitrogen uptake for most plant functional types.

3.4. Impact of Model Changes on CO_2 Fertilization and Nitrogen Deposition Responses of GPP and WUE

Both CLM4.5 and CLM4.5* show an increase in GPP with CO_2 fertilization and nitrogen deposition, with CLM4.5 having higher GPP values than CLM4.5* (Figure 6). For CLM4.5*, predicted GPP with constant 1850 CO_2 and varying nitrogen deposition (CLM4.5* + 1850 CO_2 + Ndep; black solid line) and with constant 1850 CO_2 and nitrogen deposition (CLM4.5* + 1850 CO_2 + 1850 Ndep; red solid line) remained relatively constant between 1973 and 2004. However, CLM4.5* predicted GPP with varying CO_2 fertilization and constant 1850 nitrogen deposition (CLM4.5* + CO_2 + 1850 Ndep; green solid line) increased non-linearly from 1970 to 2004 compared to GPP with constant 1850 CO_2 fertilization and nitrogen deposition (CLM4.5* + 1850 CO_2 + 1850 Ndep; red solid line) because of the non-linear increase in the rate of change of CO_2 mole fractions. Aggregated from 1973 to 2004, GPP for CLM4.5* increased by 13.1 Pg C yr^{-1}, 10.8 Pg C yr^{-1}, and 2.0 Pg C yr^{-1} with CO_2 fertilization and nitrogen deposition, CO_2 fertilization alone, and nitrogen deposition alone, respectively, compared to GPP computed with 1850 CO_2 and without nitrogen deposition.

We computed the ratio of GPP to total evapotranspiration (*WUE*) to compare with the global FLUXNET-MTE products. The spatial patterns of CLM4.5* predicted *WUE* are closer to the reference data set compared to CLM4.5, especially in the higher latitudes (Figure 7).

Table 2. ILAMB GPP, LH and LAI Scores for a Range of Metrics Aggregated Across 1995–2004 for Modified Version of CLM4.5 (CLM4.5*) and Default Version of CLM4.5 (CLM4.5)[a]

Model Name	Variable	Reference	Annual Mean	Bias	RMSE	Phase	Global Bias Score	RMSE Score	Phase Score	Taylor Score	Overall Score
CLM4.5	GPP	*Beer et al.* [2010]	138.1	19.4	5.7	0.03	0.69	0.66	0.83	0.91	0.75
CLM4.5*	GPP	*Beer et al.* [2010]	122.9	4.2	4.7	−0.1	0.74	0.71	0.85	0.9	0.78
CLM4.5	LH	*Jung et al.* [2010]	43.7	4.0	14.7	0.06	0.81	0.75	0.88	0.94	0.83
CLM4.5*	LH	*Jung et al.* [2010]	40.6	0.9	14.5	0.09	0.79	0.75	0.88	0.93	0.82
CLM4.5	LAI	*Zhu et al.* [2013]	3.1	1.6	2.1	0.44	0.49	0.45	0.72	0.51	0.52
CLM4.5*	LAI	*Zhu et al.* [2013]	2.9	1.3	1.7	0.51	0.52	0.49	0.71	0.62	0.57

[a]GPP unit for annual mean is PgC yr^{-1}, bias is PgC yr^{-1}, RMSE is PgC $month^{-1}$ and phase is months. LH unit for annual mean is W m^{-2}, bias is W m^{-2}, RMSE is W m^{-2} and phase is months. LAI unit for annual mean is m^2 m^{-2}, bias is m^2 m^{-2}, RMSE is m^2 m^{-2} and phase is months. The metric scores are unitless and range from 0 to 1.

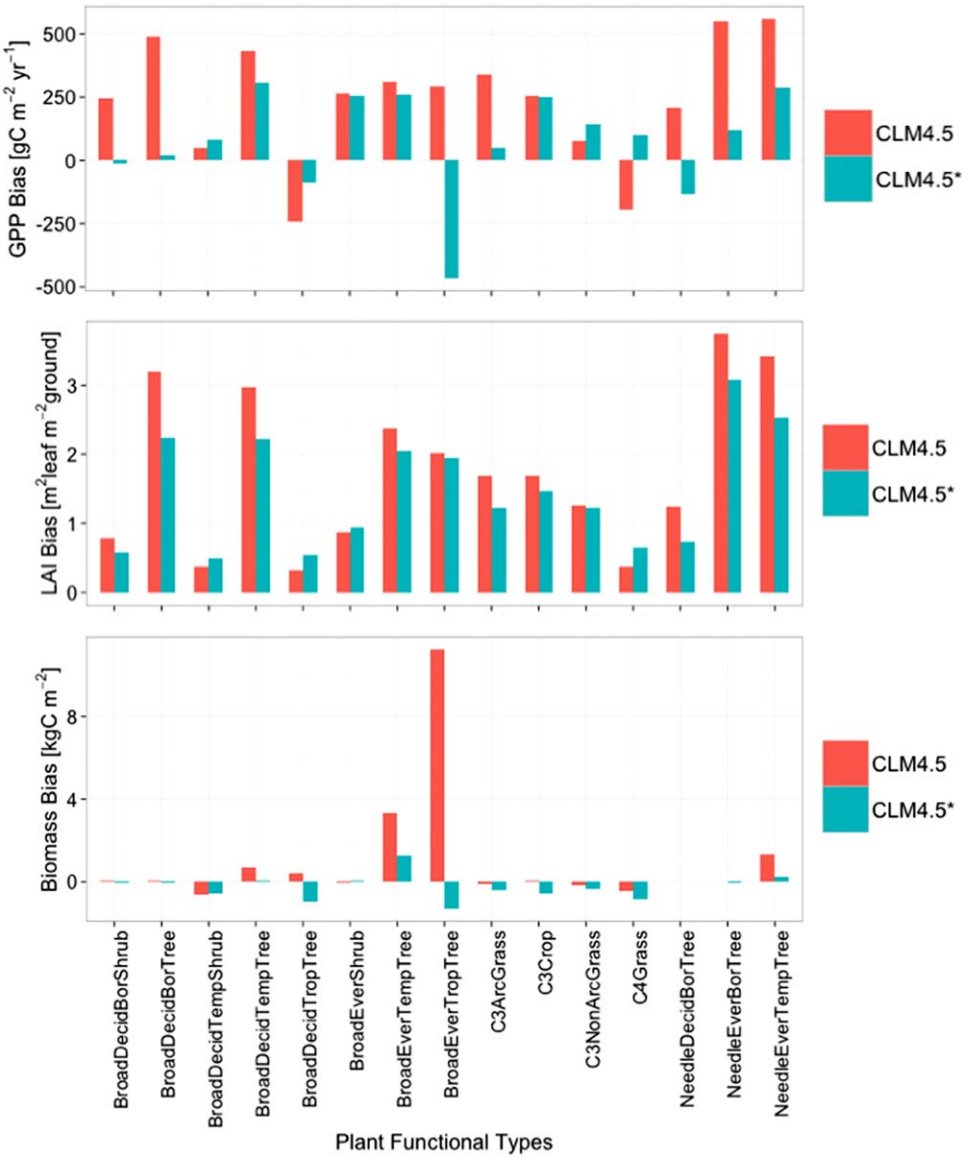

Figure 4. GPP, LAI and biomass biases (=model – reference) by plant functional types for default version of CLM4.5 (CLM4.5) and modified version of CLM4.5 (CLM4.5*). GPP and LAI biases are aggregated globally across 1995–2004, and biomass bias is computed only for the tropical regions for year 2000 due to lack of data availability at a global scale. CLM4.5* has lower bias than CLM4.5 for most plant functional types.

4. Discussion

We present a new plant model for CLM that integrates different plant nitrogen cycle mechanisms and traits important for root nutrient uptake and controls on photosynthesis. The improvements in the representation of leaf physiology in this new model structure uses actual photosynthetic parameters (as a function of leaf nitrogen) rather than potential photosynthetic parameters. We have replaced the GPP downregulation model structure in CLM4.5 (which instantaneously reduces GPP if soil mineral nitrogen is insufficient to accommodate allocation to plant tissues with fixed C:N stoichiometry) with a new model structure that scales leaf photosynthetic parameters with predicted dynamic leaf nitrogen content. We have also improved the representation of root physiology and nutrient competition by incorporating a new model structure with plant nitrogen uptake traits dependent on nitrogen uptake efficiency and root biomass.

Some previous models have also used leaf nitrogen to scale photosynthesis (e.g., CABLE, GDAY, LPJ-GUESS, OCN, SDGVM, TECO) [*Zaehle et al.*, 2014]. Other models have represented nitrogen limitation by (1)

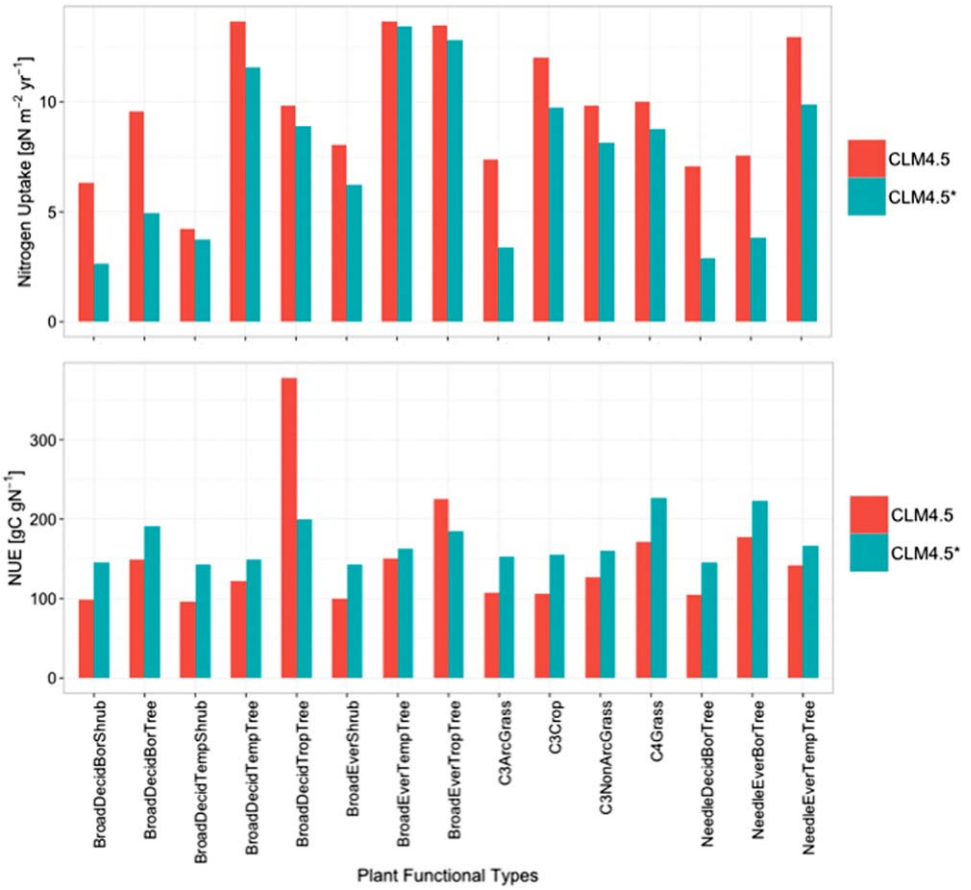

Figure 5. Plant nitrogen uptake and nitrogen use efficiency (NUE) defined as ratio of GPP and nitrogen uptake by plant functional types for default version of CLM4.5 (CLM4.5) and modified version of CLM4.5 (CLM4.5*).

prescribing a constant value for the photosynthetic parameters independent of leaf nitrogen [*Moorcroft et al*., 2001], (2) estimating GPP for conditions where nitrogen is not limiting and then downregulating GPP depending on soil nitrogen availability [*Oleson et al*., 2013], (3) accounting for the carbon costs of nutrient acquisition [*Fisher et al*., 2010], or (4) explicitly accounting for within-leaf N allocation between multiple leaf functional processes [*Ali et al*., 2015]. Our changes to leaf physiology in CLM4.5 are based on recent studies that have shown that photosynthetic parameters strongly scale with leaf nitrogen across a diverse range of plant functional types [*Kattge et al*., 2009]. In our model, we have used the plant functional type specific relationship of photosynthetic parameters to leaf nitrogen to incorporate the range of variation across different plant species. However, we need to further improve the representation of tropical plant functional types, which have high species diversity due to variations in soil conditions (e.g., oxisols versus non-oxisols), successional dynamics and stand structure, species adaption, and forest management. This improvement in representing tropical plant functional types can be performed by incorporating additional plant functional types and processes to represent the diversity of ecosystems in the tropics. We note that our method described here is compatible with some additional C-N coupling processes, e.g., those of *Fisher et al*. [2010] and *Ali et al*. [2015], which are being included in the upcoming CLM5.

We have also improved the representation of root physiology by incorporating a model structure with plant nitrogen uptake proportional to nitrogen uptake efficiency and root biomass. This new representation of root physiology is based on a mathematical formulation that incorporates the Michaelis-Menten reaction kinetics similar to that implemented by *Zaehle and Friend* [2010] and *Thomas et al*. [2013]. The inclusion of a model structure with nitrogen uptake relying on root processes is more consistent with theoretical and empirical understanding of the controls of root surface area, ionic diffusion gradients, and transporter molecules on root nitrogen uptake [*Miller and Cramer*, 2005; *Pate*, 1973]. These controls on root nitrogen uptake

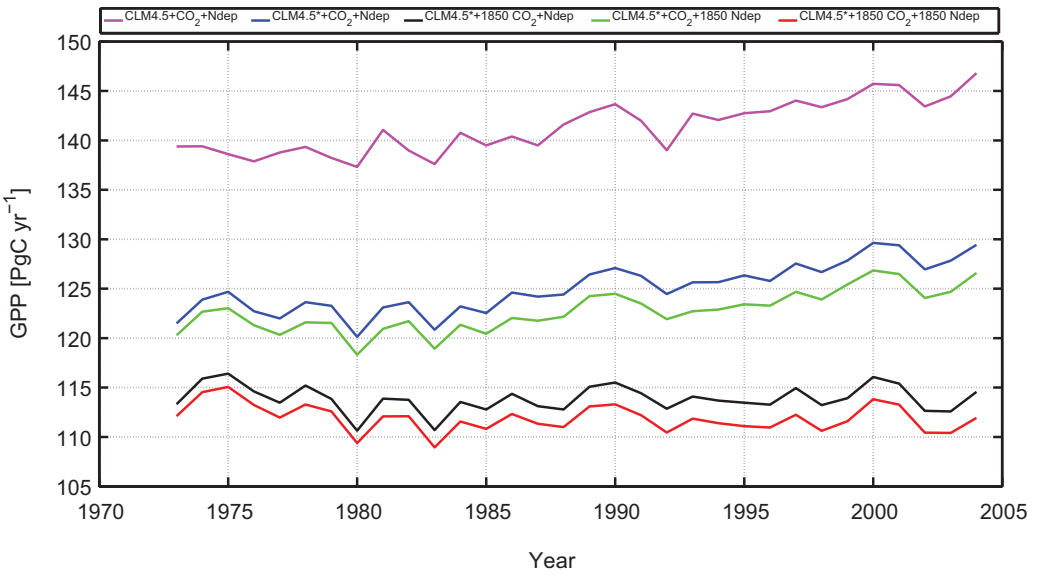

Figure 6. Historical response of global GPP to CO_2 fertilization and nitrogen deposition for CLM4.5* and CLM4.5. Both CLM4.5 and CLM4.5* show an increase in GPP with CO_2 fertilization and nitrogen deposition with CLM4.5 having higher GPP values than CLM4.5*. Legend captions: CLM4.5* + 1850 CO_2 + 1850 Ndep (red solid line) is predicted GPP with constant 1850 CO_2 and nitrogen deposition for CLM4.5*; CLM4.5* + 1850 CO_2 + Ndep (black solid line) is predicted GPP with constant 1850 CO_2 and varying nitrogen deposition for CLM4.5*; CLM4.5* + CO_2 + 1850 Ndep (green solid line) is predicted GPP with varying CO_2 fertilization and constant 1850 nitrogen deposition for CLM4.5*; CLM4.5* + CO_2 + Ndep (blue solid line) is predicted GPP with varying CO_2 fertilization and nitrogen deposition for CLM4.5*; CLM4.5 + CO_2 + Ndep (magenta solid line) is predicted GPP with varying CO_2 fertilization and nitrogen deposition for CLM4.5.

in CLM4.5* are represented by root biomass and maximum nitrogen uptake parameters. In doing so, we assume that root biomass is proportional to root surface area and maximum nitrogen uptake represents the role of ionic diffusion gradients and transporter molecules in nitrogen uptake. Future work will investigate the value of explicitly representing these controls on root uptake kinetics.

The improved model structure also incorporates a flexible leaf carbon to nitrogen ratio. Although the flexible carbon to nitrogen ratio is an improvement over a fixed ratio, we have simplified the complex interactions between carbon and nitrogen cycling in plants by imposing maximum and minimum bounds to this ratio. An improvement to our current approach would consist of a completely prognostic carbon to nitrogen ratio without maximum and minimum bounds where the carbon to nitrogen ratio would emerge from the interactions of the carbon and nitrogen cycles in plants [*Grant et al*., 2010; *Thomas and Williams*, 2014]. A completely prognostic carbon to nitrogen ratio is beyond the scope of this study and is an area of future research.

LAI and biomass predictions in CLM4.5 are not only influenced by GPP and autotrophic respiration but also by vegetation turnover and allocation. The parameters for representing the dynamics of vegetation turnover and allocation are uncertain in models because these parameters are not estimated from a representative global sample. The uncertainties in these parameters can be reduced by using global data sets (e.g., TRY) [*Kattge et al*., 2011] for parameterizing vegetation turnover and carbon and nitrogen allocation. However the use of these data products is not straightforward because of the limited quantity of globally representative samples (e.g., for carbon allocation), lack of observations that can directly translate to models (e.g., lack of data on vertical canopy specific leaf area (SLA) profiles), sampling biases (due to sampling at targeted locations as opposed to globally representative samples), and large variability in the synthesized data leading to large variability across similar plant functional types.

The new model simulations produced lower global GPP bias (compared to the *Beer et al*. [2010] FLUXNET-MTE reference data set) of 41 gC m^{-2} yr^{-1} compared to a global GPP bias of 138 gC m^{-2} yr^{-1} predicted by CLM4.5 during the same time period. CLM 4.5*'s GPP biases vary by region with some regions (e.g., Europe and North America) having lower bias compared to CLM4.5 than other regions (e.g., Australia). CLM4.5* also produced lower LAI and biomass biases compared to CLM4.5 with respect to reference data. We note that the reference data sets we used to evaluate the predicted GPP distributions are themselves uncertain, since

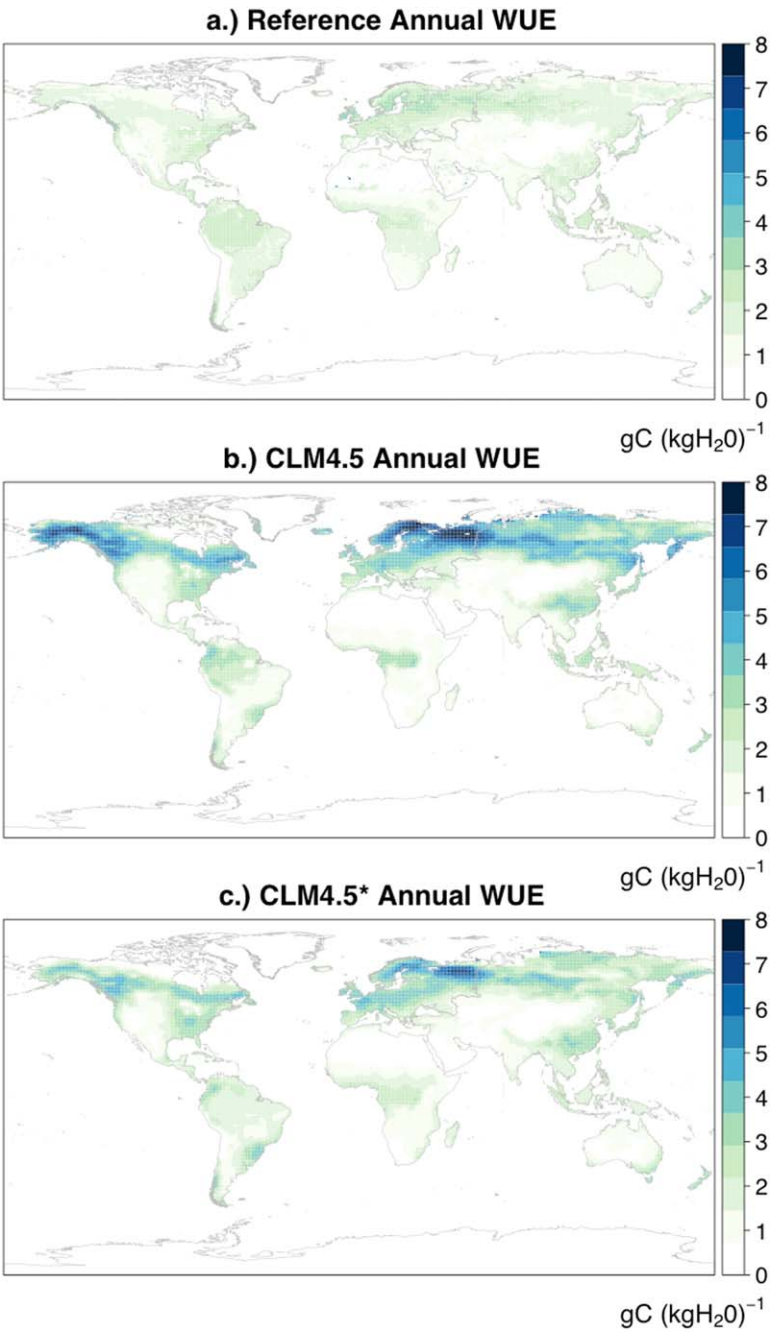

Figure 7. Spatial distribution of annual WUE_{ET} (ratio of GPP to evapotranspiration) for (a) reference data, (b) default version of CLM4.5 (CLM4.5), and (c) modified version of CLM4.5 (CLM4.5*) aggregated across 1995–2004. The spatial patterns of CLM4.5* predicted *WUE* are lower and closer to the reference data set compared to CLM4.5, especially in the higher latitudes.

they are based on applying a simple model to in-situ observations, and then extrapolating those predictions using re-analysis climate forcing data. For example, the FLUXNET-MTE GPP data product is derived by integrating flux tower net ecosystem exchange (NEE) observations with modeled ecosystem respiration and a machine learning algorithm.

The new model structure in CLM4.5* removes the limitations of the CLM4.5 instantaneous nitrogen down-regulation framework, which causes unrealistic dips in GPP diurnal cycles caused by unrealistic midday soil mineral nitrogen depletion. The new model structure prognoses the photosynthesis-nitrogen relationship and buffers the effect of fluctuations in the supply of nitrogen for photosynthesis. Nonetheless, we note

that many qualitative behaviors of the model are similar between the new and old structures, e.g., GPP and WUE increase in response to elevated CO_2 and nitrogen deposition. Thus, many key model predictions concerning carbon cycle responses to global change are qualitatively robust with respect to differing mechanistic representation of leaf carbon-nitrogen coupling.

Most land models impose fixed C:N ratios for different plant parts to represent the effect of nitrogen limitation on plant productivity. However, a few land models (e.g., O-CN) predict dynamic C:N ratios based on carbon and nitrogen allocation to plant growth. The new model structure in CLM4.5* allows us to predict a dynamic C:N ratio, and determine the influence of climate, nutrient availability, and CO_2 fertilization on this ratio. However, we found unrealistically high C:N ratio for broadleaf deciduous boreal shrub and C_4 grass plant functional types in CLM4.5*. We hypothesize that these values are related to either lower mortality rates for these plant functional types in CLM, or the high slope of the V_{cmax} and leaf nitrogen relationship in the TRY database, which causes higher photosynthesis and carbon accumulation for a given amount of leaf nitrogen. This high slope could be related to biases in the TRY database, which is based on targeted sampling at particular locations (as opposed to random sampling globally across different biomes), or lack of one-to-one correspondence between plant functional types defined in CLM and those reported in *Kattge et al*. [2009]. Future work will focus on further improving the representation of mortality rates and the V_{cmax} and leaf nitrogen relationship in CLM4.5*.

Our current model developments motivate several future areas of research in improving the representation of nitrogen cycling in models. We would like to investigate how the seasonal phases of different processes differ between CLM4.5 and CLM4.5*. We also intend to incorporate dynamic carbon and nitrogen allocation (as opposed to fixed allocation) by integrating effects of resource availability and allometric constraints. Another area of future research relates to incorporating the costs and investment of plant carbon in acquiring, transporting, and storing nutrients including active nitrogen uptake, passive nitrogen uptake, nutrient retranslocation, nitrogen fixation, and mycorrhizal association. Another area of research relates to the competition for nitrogen amongst different consumers (e.g., plants and microbial immobilization) and nitrogen transformations (e.g., nitrification, denitrification, and leaching) in the model. In most land surface models that include nitrogen cycling, this competition is determined based on a relative demand and supply approach whereby nitrogen is partitioned to different consumers and transformations either in series, where one consumer takes up nitrogen based on its demand with the residual available to other consumers, or in parallel by simultaneously partitioning the supply based on the relative demands of different consumers and transformations. An improved alternative to partitioning nitrogen supply would rely on ECA kinetics [*Tang and Riley*, 2013, 2015; *Zhu and Riley*, 2015; *Zhu et al*., 2015] that improves on the Michaelis Menten kinetics by incorporating competition amongst multiple consumers for multiple substrates.

In this study, we have assessed carbon cycling. However, land surface processes can also feedback to climate via changes in evapotranspiration and albedo [*Bonan*, 2008]. The net climate impact of land surface processes is spatially heterogeneous and depends on the net balance of carbon and nitrogen trace-gases, evapotranspiration, and albedo feedbacks, all of which are strongly coupled with atmospheric processes. Further work is needed for a comprehensive assessment of the impact of land surface feedbacks via carbon, energy, and water cycles using a fully coupled ESM framework.

5. Conclusion

This study presents improvements in modeling leaf and root physiology and nitrogen allocation in CLM4.5. The model structural improvements in leaf physiology use global relationships for leaf nitrogen and photosynthetic traits (e.g., V_{cmax}). These improvements replace the GPP downregulation model framework that reduces GPP if nitrogen is limiting. In the new CLM4.5* model structure, nitrogen impacts on GPP are predicted directly with leaf nitrogen content, which is affected by root traits that affect plant nitrogen uptake. The representation of root physiology was improved by incorporating root traits related to nitrogen uptake efficiency and root biomass, and using Michaelis-Menten reaction kinetics to represent root and microbe competition. The new model structure also incorporates a flexible carbon to nitrogen ratio, and improved carbon allocation for tropical regions that is consistent with field-based data [*Malhi et al*., 2011].

We evaluated the model against multiple reference data sets for GPP, LAI, and biomass and a wide suite of metrics using the ILAMB package. CLM4.5* has lower bias for GPP, LAI, and biomass compared to the

baseline version of CLM4.5. The mechanistic representation of leaf-level nitrogen allocation and a theoretically consistent treatment of plant nitrogen uptake lead to overall improvements in CLM4.5's global carbon cycling predictions. Several follow-on research areas are described, including incorporating dynamic carbon and nitrogen allocation, carbon costs of nutrient acquisition, mechanistic representation of plant and microbial competition for nutrients, and optimal allocation of leaf nitrogen for sub-processes in photosynthesis and respiration.

Acknowledgments
This research was supported by the Director, Office of Science, Office of Biological and Environmental Research of the US Department of Energy under Contract DE-AC02-05CH11231 as part of the NGEE-Arctic, BGC-Climate Feedbacks, and ACME projects. The data used in this paper can be obtained by contacting the first author at bghimire@lbl.gov.

References

Ali, A. A., et al. (2015), A global scale mechanistic model of the photosynthetic capacity, *Geosci. Model Dev. Discuss.*, *8*(8), 6217–6266, doi: 10.5194/gmdd-8-6217-2015.

Beer, C., M. Reichstein, E. Tomelleri, P. Ciais, M. Jung, N. Carvalhais, C. Rödenbeck, M. A. Arain, D. Baldocchi, and G. B. Bonan (2010), Terrestrial gross carbon dioxide uptake: Global distribution and covariation with climate, *Science*, *329*(5993), 834–838.

Bonan, G. (2008), Forests and climate change: Forcings, feedbacks, and the climate benefits of forests, *Science*, *320*(5882), 1444–1449.

Bonan, G. B., P. J. Lawrence, K. W. Oleson, S. Levis, M. Jung, M. Reichstein, D. M. Lawrence, and S. C. Swenson (2011), Improving canopy processes in the Community Land Model version 4 (CLM4) using global flux fields empirically inferred from FLUXNET data, *J. Geophys. Res.*, *116*, G02014, doi:10.1029/2010JG001593.

Evans, J. R. and J. R. Seemann (1989a), The allocation of protein nitrogen in the photosynthetic apparatus: Cost, consequences, and control, in edited by W. R. Briggs, pp. 183–205, Photosynthesis, Alan R. Liss, Inc., N. Y.

Evans, J. (1989b), Photosynthesis and nitrogen relationships in leaves of C3 plants, *Oecologia*, *78*(1), 9–19.

Farquhar, G., S. v. von Caemmerer, and J. Berry (1980), A biochemical model of photosynthetic CO2 assimilation in leaves of C3 species, *Planta*, *149*(1), 78–90.

Fisher, J. B., S. Sitch, Y. Malhi, R. A. Fisher, C. Huntingford, and S.-Y. Tan (2010), Carbon cost of plant nitrogen acquisition: A mechanistic, globally applicable model of plant nitrogen uptake, retranslocation, and fixation, *Global Biogeochem. Cycles*, *24*, GB1014, doi:10.1029/2009GB003621.

Foley, J., S. Levis, I. C. Prentice, D. Pollard, and S. L. Thompson (1998), Coupling dynamic models of climate and vegetation, *Global Change Biol.*, *4*(5), 561–579.

Friedlingstein, P., P. Cox, R. Betts, L. Bopp, W. Von Bloh, V. Brovkin, P. Cadule, S. Doney, M. Eby, and I. Fung (2006), Climate-carbon cycle feedback analysis: Results from the C4MIP model intercomparison, *J. Clim.*, *19*(14), 3337–3353.

Grant, R., A. Barr, T. Black, H. Margolis, J. McCaughey, and J. Trofymow (2010), Net ecosystem productivity of temperate and boreal forests after clearcutting—A Fluxnet-Canada measurement and modelling synthesis, *Tellus, Ser. B*, *62*(5), 475–496.

Gregory, J. M., C. Jones, P. Cadule, and P. Friedlingstein (2009), Quantifying carbon cycle feedbacks, *J. Clim.*, *22*(19), 5232–5250.

Hu, S., F. S. Chapin, M. Firestone, C. Field, and N. Chiariello (2001), Nitrogen limitation of microbial decomposition in a grassland under elevated CO2, *Nature*, *409*(6817), 188–191.

Huntzinger, D., C. Schwalm, A. Michalak, K. Schaefer, A. King, Y. Wei, A. Jacobson, S. Liu, R. Cook, and W. Post (2013), The north american carbon program multi-scale synthesis and terrestrial model intercomparison project-–Part 1: Overview and experimental design, *Geosci. Model Dev.*, *6*(6), 2121–2133.

Hurtt, G., S. Frolking, M. Fearon, B. Moore, E. Shevliakova, S. Malyshev, S. Pacala, and R. Houghton (2006), The underpinnings of land-use history: Three centuries of global gridded land-use transitions, wood-harvest activity, and resulting secondary lands, *Global Change Biol.*, *12*(7), 1208–1229.

Jonasson, S., A. Michelsen, and I. K. Schmidt (1999), Coupling of nutrient cycling and carbon dynamics in the Arctic, integration of soil microbial and plant processes, *Appl. Soil Ecol.*, *11*(2), 135–146.

Jung, M., M. Reichstein, P. Ciais, S. I. Seneviratne, J. Sheffield, M. L. Goulden, G. Bonan, A. Cescatti, J. Chen, and R. De Jeu (2010), Recent decline in the global land evapotranspiration trend due to limited moisture supply, *Nature*, *467*(7318), 951–954.

Kattge, J., and W. Knorr (2007), Temperature acclimation in a biochemical model of photosynthesis: A reanalysis of data from 36 species, *Plant Cell Environ.*, *30*(9), 1176–1190.

Kattge, J., W. Knorr, T. Raddatz, and C. Wirth (2009), Quantifying photosynthetic capacity and its relationship to leaf nitrogen content for global-scale terrestrial biosphere models, *Global Change Biol.*, *15*(4), 976–991.

Kattge, J., S. Diaz, S. Lavorel, I. Prentice, P. Leadley, G. Bönisch, E. Garnier, M. Westoby, P. B. Reich, and I. Wright (2011), TRY—A global database of plant traits, *Global Change Biol.*, *17*(9), 2905–2935.

Kaye, J. P., and S. C. Hart (1997), Competition for nitrogen between plants and soil microorganisms, *Trends Ecol. Evol.*, *12*(4), 139–143.

Koven, C., W. Riley, Z. Subin, J. Tang, M. Torn, W. Collins, G. Bonan, D. Lawrence, and S. Swenson (2013), The effect of vertically resolved soil biogeochemistry and alternate soil C and N models on C dynamics of CLM4, *Biogeosciences*, *10*(11), 7109–7131.

Lamarque, J. F., et al. (2005), Assessing future nitrogen deposition and carbon cycle feedback using a multimodel approach: Analysis of nitrogen deposition, *J. Geophys. Res.*, *110*, D19303, doi:10.1029/2005JD005825.

LeBauer, D. S., and K. K. Treseder (2008), Nitrogen limitation of net primary productivity in terrestrial ecosystems is globally distributed, *Ecology*, *89*(2), 371–379.

Luo, Y., J. T. Randerson, G. Abramowitz, C. Bacour, E. Blyth, N. Carvalhais, P. Ciais, D. Dalmonech, J. B. Fisher, and R. Fisher (2012), A framework for benchmarking land models, *Biogeosciences*, *9*(10), 3857–3874.

Makino, A., and B. Osmond (1991), Effects of nitrogen nutrition on nitrogen partitioning between chloroplasts and mitochondria in pea and wheat, *Plant Physiol.*, *96*(2), 355–362.

Malhi, Y., C. Doughty, and D. Galbraith (2011), The allocation of ecosystem net primary productivity in tropical forests, *Philos. Trans. R. Soc. B*, *366*(1582), 3225–3245.

Matson, P., K. A. Lohse, and S. J. Hall (2002), The globalization of nitrogen deposition: Consequences for terrestrial ecosystems, *Ambio*, *31*(2), 113–119.

McCormack, M. L., I. A. Dickie, D. M. Eissenstat, T. J. Fahey, C. W. Fernandez, D. Guo, H. S. Helmisaari, E. A. Hobbie, C. M. Iversen, and R. B. Jackson (2015), Redefining fine roots improves understanding of below-ground contributions to terrestrial biosphere processes, *New Phytol.*, *207*, 505–518.

McMurtrie, R. E., C. M. Iversen, R. C. Dewar, B. E. Medlyn, T. Näsholm, D. A. Pepper, and R. J. Norby (2012), Plant root distributions and nitrogen uptake predicted by a hypothesis of optimal root foraging, *Ecol. Evol.*, *2*(6), 1235–1250.

Michaelis, L., and M. L. Menten (1913), Die kinetik der invertinwirkung, *Biochem. Z*, *49*(333–369), 352.
Miller, A., and M. Cramer (2005), Root nitrogen acquisition and assimilation, in *Root Physiology: From Gene to Function*, edited by H. Lambers and T. D. Colmer, pp. 1–36, Springer, Netherlands.
Moorcroft, P., G. Hurtt, and S. W. Pacala (2001), A method for scaling vegetation dynamics: The ecosystem demography model (ED), *Ecol. Monogr.*, *71*(4), 557–586.
Oleson, K., D. Lawrence, G. Bonan, B. Drewniak, M. Huang, C. Koven, S. Levis, F. Li, W. Riley, and Z. Subin (2013), Technical description of version 4.5 of the Community Land Model (CLM), *NCAR Tech Rep. Note NCAR/TN-503+ STR*, 422 pp., Natl. Cent. for Atmos. Res., Boulder, Colo., doi:10.5065/D6RR1W7M.
Pate, J. (1973), Uptake, assimilation and transport of nitrogen compounds by plants, *Soil Biol. Biochem.*, *5*(1), 109–119.
Qian, T., A. Dai, K. E. Trenberth, and K. W. Oleson (2006), Simulation of global land surface conditions from 1948 to 2004. Part I: Forcing data and evaluations, *J. Hydrometeorol.*, *7*(5), 953–975.
Read, D., and J. Perez-Moreno (2003), Mycorrhizas and nutrient cycling in ecosystems––A journey towards relevance?, *New Phytol.*, *157*(3), 475–492.
Reich, P. B., M. B. Walters, and D. S. Ellsworth (1997), From tropics to tundra: Global convergence in plant functioning, Proc. *Natl. Acad. Sci. U. S. A.*, *94*(25), 13,730–13,734.
Reich, P. B., S. E. Hobbie, T. Lee, D. S. Ellsworth, J. B. West, D. Tilman, J. M. Knops, S. Naeem, and J. Trost (2006), Nitrogen limitation constrains sustainability of ecosystem response to CO2, *Nature*, *440*(7086), 922–925.
Riley, W., Z. Subin, D. Lawrence, S. Swenson, M. Torn, L. Meng, N. Mahowald, and P. Hess (2011), Barriers to predicting changes in global terrestrial methane fluxes: Analyses using CLM4Me, a methane biogeochemistry model integrated in CESM, *Biogeosciences*, *8*(7), 1925–1953.
Rogers, A. (2014), The use and misuse of V c, max in Earth System Models, *Photosynthesis Res.*, *119*(1–2), 15–29.
Saatchi, S. S., N. L. Harris, S. Brown, M. Lefsky, E. T. Mitchard, W. Salas, B. R. Zutta, W. Buermann, S. L. Lewis, and S. Hagen (2011), Benchmark map of forest carbon stocks in tropical regions across three continents, *Proc. Natl. Acad. Sci. U. S. A.*, *108*(24), 9899–9904.
Schaefer, K., et al. (2012), A model-data comparison of gross primary productivity: Results from the North American Carbon Program site synthesis, *J. Geophys. Res.*, *117*, G03010, doi:10.1029/2012JG001960.
Sellers, P., Y. Mintz, Y. E. A. Sud, and A. Dalcher (1986), A simple biosphere model (SiB) for use within general circulation models, *J. Atmos. Sci.*, *43*(6), 505–531.
Sitch, S., B. Smith, I. C. Prentice, A. Arneth, A. Bondeau, W. Cramer, J. Kaplan, S. Levis, W. Lucht, and M. T. Sykes (2003), Evaluation of ecosystem dynamics, plant geography and terrestrial carbon cycling in the LPJ dynamic global vegetation model, *Global Change Biol.*, *9*(2), 161–185.
Smithwick, E. A., M. S. Lucash, M. L. McCormack, and G. Sivandran (2014), Improving the representation of roots in terrestrial models, *Ecol. Modell.*, *291*, 193–204.
Tang, J., and W. Riley (2013), A total quasi-steady-state formulation of substrate uptake kinetics in complex networks and an example application to microbial litter decomposition, *Biogeosciences*, *10*(12), 8329–8351.
Tang, J., and W. Riley (2015), Weaker soil carbon-climate feedbacks resulting from microbial and abiotic interactions, *Nat. Clim. Change*, *5*(1), 56–60.
Thomas, R., and M. Williams (2014), A model using marginal efficiency of investment to analyze carbon and nitrogen interactions in terrestrial ecosystems, Geoscientific Model Development, *7*, 2015–2037.
Thomas, R., G. Bonan, and C. Goodale (2013), Insights into mechanisms governing forest carbon response to nitrogen deposition: A model–data comparison using observed responses to nitrogen addition, *Biogeosciences*, *10*(6), 3869–3887.
Thornton, P., and N. E. Zimmermann (2007), An improved canopy integration scheme for a land surface model with prognostic canopy structure, *J. Clim.*, *20*(15), 3902–3923.
Thornton, P., J.-F. Lamarque, N. A. Rosenbloom, and N. M. Mahowald (2007), Influence of carbon-nitrogen cycle coupling on land model response to CO2 fertilization and climate variability, *Global Biogeochem. Cycles*, *21*, GB4018, doi:10.1029/2006GB002868.
Thornton, P., S. C. Doney, K. Lindsay, J. K. Moore, N. Mahowald, J. T. Randerson, I. Fung, J.-F. Lamarque, J. J. Feddema, and Y.-H. Lee (2009), Carbon-nitrogen interactions regulate climate-carbon cycle feedbacks: Results from an atmosphere-ocean general circulation model, *Biogeosciences*, *6*(10), 2099–2120.
Vitousek, P. M., and R. W. Howarth (1991), Nitrogen limitation on land and in the sea: How can it occur?, *Biogeochemistry*, *13*(2), 87–115.
Wang, Y., R. Law, and B. Pak (2010), A global model of carbon, nitrogen and phosphorus cycles for the terrestrial biosphere, *Biogeosciences*, *7*(7), 2261–2282.
Warren, J. M., P. J. Hanson, C. M. Iversen, J. Kumar, A. P. Walker, and S. D. Wullschleger (2015), Root structural and functional dynamics in terrestrial biosphere models—Evaluation and recommendations, *New Phytol.*, *205*(1), 59–78.
Zaehle, S., and A. Friend (2010), Carbon and nitrogen cycle dynamics in the O-CN land surface model: 1. Model description, site-scale evaluation, and sensitivity to parameter estimates, *Global Biogeochem. Cycles*, *24*, GB1005, doi:10.1029/2009GB003521.
Zaehle, S., B. E. Medlyn, M. G. De Kauwe, A. P. Walker, M. C. Dietze, T. Hickler, Y. Luo, Y. P. Wang, B. El-Masri, and P. Thornton (2014), Evaluation of 11 terrestrial carbon–nitrogen cycle models against observations from two temperate Free-Air CO2 Enrichment studies, *New Phytol.*, *202*(3), 803–822.
Zhu, Q., and W. Riley (2015), Improved modelling of soil nitrogen losses, *Nat. Clim. Change*, *5*, 705–706.
Zhu, Q., W. Riley, J. Tang, and C. Koven (2015), Multiple soil nutrient competition between plants, microbes, and mineral surfaces: Model development, parameterization, and example applications in several tropical forests, *Biogeosci. Discuss.*, *12*(5), 4057–4106.
Zhu, Z., J. Bi, Y. Pan, S. Ganguly, A. Anav, L. Xu, A. Samanta, S. Piao, R. R. Nemani, and R. B. Myneni (2013), Global data sets of vegetation leaf area index (LAI) 3g and Fraction of Photosynthetically Active Radiation (FPAR) 3g derived from Global Inventory Modeling and Mapping Studies (GIMMS) Normalized Difference Vegetation Index (NDVI3g) for the period 1981 to 2011, *Remote Sens.*, *5*(2), 927–948.